

VisionReward: Fine-Grained Multi-Dimensional Human Preference Learning for Image and Video Generation

Jiazheng Xu^{1*} Yu Huang^{1*} Jiale Cheng¹ Yuanming Yang¹ Jiajun Xu¹ Yuan Wang¹
 Wenbo Duan¹ Shen Yang¹ Qunlin Jin¹ Shurun Li¹ Jiayan Teng¹ Zhuoyi Yang¹
 Wendi Zheng¹ Xiao Liu¹ Ming Ding² Xiaohan Zhang² Xiaotao Gu² Shiyu Huang²
 Minlie Huang¹ Jie Tang¹ Yuxiao Dong¹

¹Tsinghua University ²Zhipu AI

Abstract

Visual generative models have achieved remarkable progress in synthesizing photorealistic images and videos, yet aligning their outputs with human preferences across critical dimensions remains a persistent challenge. Though reinforcement learning from human feedback offers promise for preference alignment, existing reward models for visual generation face limitations, including black-box scoring without interpretability and potentially resultant unexpected biases. We present VisionReward, a general framework for learning human visual preferences in both image and video generation. Specifically, we employ a hierarchical visual assessment framework to capture fine-grained human preferences, and leverages linear weighting to enable interpretable preference learning. Furthermore, we propose a multi-dimensional consistent strategy when using VisionReward as a reward model during preference optimization for visual generation. Experiments show that VisionReward can significantly outperform existing image and video reward models on both machine metrics and human evaluation. Notably, VisionReward surpasses VideoScore by 17.2% in preference prediction accuracy, and text-to-video models with VisionReward achieve a 31.6% higher pairwise win rate compared to the same models using VideoScore. All code and datasets are provided at <https://github.com/THUDM/VisionReward>.

1. Introduction

Visual generative models, including text-to-image [2, 9, 31, 33–35] and text-to-video [4, 15, 17, 42, 50, 54] generation, have recently experienced rapid developments. Through

*Equal contributions. {xjz22, h-y22}@mails.tsinghua.edu.cn

Core contributors: Jiazheng, Yu, Jiale, Yuanming, Jiajun, Yuan, Wenbo and Shen.

large-scale pretraining, these models can effectively translate textual descriptions into photorealistic images or temporally coherent videos. To further align them with human preferences, reinforcement learning from human feedback (RLHF) [30]—initially introduced in large language models—has recently been adapted to visual generation tasks [12, 49].

A key bottleneck in applying RLHF to visual generation lies in developing effective visual reward models. Recent studies [22, 47, 49] have explored training reward models to predict human visual preferences, enabling automatic evaluation and preference optimization for visual generative models. For evaluation, reward models function as automated metrics that quantitatively measure the alignment between generated outputs and human preference criteria [23]. For optimization, reward models identify reliable directions for improving visual generation models. Essentially, they can provide feedback in reinforcement learning or generate preference pairs, thus reducing dependence on human annotation [3, 7, 10].

Despite recent progress in reward models (RMs) for visual generation, two primary challenges remain: First, *lack of interpretability and risk of unexpected bias*. Current RMs [22, 47, 49] for visual generation often suffer from limited interpretability. These models inherently involve complex trade-offs among multiple factors, yet their scoring mechanisms lack transparency regarding how such trade-offs are quantified and balanced. This opacity raises concerns about *potential unexpected biases*. Though multi-modal LLMs like Gemini [41] and GPT-4o [1] enhance interpretability through explainable rating rationales, their general-purpose architectures usually underperform specialized black-box models in fine-grained technical assessments [6]. This raises a key dilemma: how to design new preference prediction methods that allow preference prediction to be interpretable while maintaining accuracy.

a) VisionReward for Text-to-Video Evaluation

Text: A child is eating pizza.



VisionReward (Ours)	
Question: Is smoothness of object's movement good?	Answer: Yes
	Answer: No

Question: Are the details relatively refined?	Answer: Yes
	Answer: No

.....	
Linear Weighted Sum of Binary VQA	
3.71 ✔	>
2.91	

VideoScore	
2.76	<
3.33 ✘	

b) VisionReward for Text-to-Video Optimization

Text: In a dimly lit, ancient library, Sarah, a young woman with fiery red hair, pores over an old book, whispering an incantation.



Original



DPO with VideoScore



DPO with VisionReward (Ours)

Figure 1. Illustration of how VisionReward works for evaluation and optimization of visual generation. a) **Evaluation**: VisionReward performs comprehensive evaluation through dimension-specific binary visual QA testing, producing human-aligned, fine-grained assessment scores. b) **Optimization**: VisionReward enable better preference optimization, enhancing multiple key aspects.

Second, *lack of effective reward models for video generation*. The rapid development of text-to-video generative models has intensified the demand for video reward models, yet this crucial component remains underdeveloped to date. Although image reward models can assess individual frame quality, their frame-level nature inherently neglects essential temporal dependencies in video sequences. While VideoScore [12] has pioneered direct video evaluation through learnable metrics, it still suffers from limitations such as insufficient accuracy in preference prediction and optimization in video generation.

Contribution. To address these challenges, we propose a general framework VisionReward to build accurate reward models for both image and video generation. VisionReward is trained with two steps: *fine-grained visual assessment* and *interpretable preference learning*. First, to capture human visual preferences, we identify nine major dimensions and decouple preferences into 64 fine-grained questions. Second, to ensure interpretable preference learning, we propose to use the classical linear weighting mechanism on the question outcomes. It enables intuitive visualization of each question's impact.

To apply it as a reward model for visual generation models, we propose a *multi-dimensional consistent strategy* during preference optimization. The goal of this strategy is to mitigate unintended and unquantifiable biases. Specifically, a pair of visual samples is used for preference optimization

(e.g., DPO [43]) only if one sample is consistently preferred over the other across all nine dimensions above.

Note that existing approaches [25, 52] have attempted to augment human annotations or expand dimensions of human preferences in visual generation. Different from them, VisionReward defines multi-dimensional human preferences with the goal of 1) disentangling distinct factors to decouple human preferences and 2) thus identifying consistently-preferred samples across all dimensions for preference optimization.

To summarize, we present VisionReward as a general framework for visual preference learning. Empirically, we show that VisionReward makes the following contributions:

- For visual preference prediction, VisionReward achieves state-of-the-art performance across multiple benchmarks, while maintaining interpretability via hierarchical diagnostic QA and explicit linear weighting. For instance, VisionReward outperforms VideoScore [12] by 17.2% in accuracy on the human preference prediction task.
- For visual generation, VisionReward can serve as an effective reward model for preference optimization (e.g., DPO), significantly enhancing the text-to-image and text-to-video models. For example, video generation models with VisionReward achieve a 31.6% higher pairwise win rate compared to the same models using VideoScore.

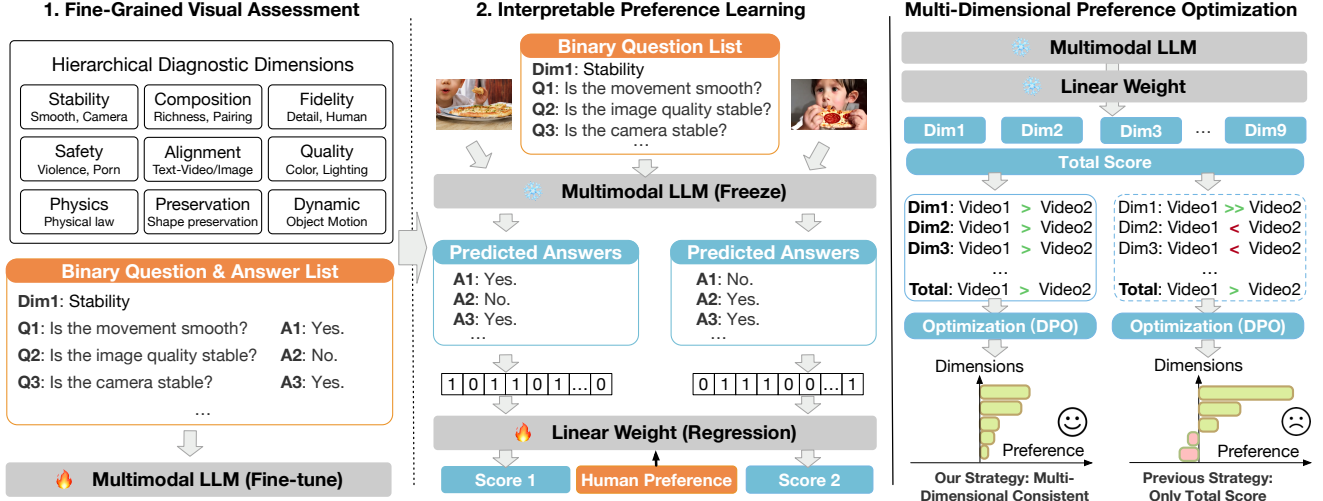


Figure 2. Overall framework of VisionReward. 1) Fine-grained Visual Assessment: fine-tune multimodal LLM to perform binary visual question-answering through hierarchical dimensions. 2) Interpretable Preference Learning: utilize visual QA outputs to predict preferences through linear weighted summation. 3) Multi-Dimensional Preference Optimization: optimization strategy across multiple dimensions.

2. VisionReward

The complete training process of VisionReward and its application methodology during preference optimization are illustrated in Fig. 2. The training of VisionReward comprises two synergistic stages:

- **Fine-grained Visual Assessment:** we develop a hierarchical framework and fine-tune the visual language model to obtain accurate visual assessment capability.
- **Interpretable Preference Learning:** Leveraging the fine-tuned visual language model, we convert its results into binary entries and apply linear regression to learn the optimal weight for predicting preferences.

2.1. Fine-grained Visual Assessment

Hierarchical Diagnostic Framework. When evaluating an image or video, human preferences are often a result of the interplay of multiple factors, necessitating a balance among various considerations. To deconstruct human preferences systematically, we develop a hierarchical diagnostic framework across multiple dimensions (e.g., text alignment, fidelity, safety). Each dimension is operationalized through binary questions requiring yes/no responses. There are 5 dimensions and 61 binary questions for text-to-image, while 9 dimensions and 64 binary questions for text-to-video.

Dataset Annotation. To ensure diversity in our annotated data, we sample from various data sources, preparing 48K images and 33K videos for annotation. Through specialized annotation, we obtain an image dataset containing **3 million** question-answer pairs and a video dataset with **2 million** pairs (Cf. Appendix Sec. 7 and Sec. 10 for details).

Visual Instruction Tuning.

Specifically, we use CogVLM2 [18] as the base model for image understanding, and CogVLM2-Video [18] as the base model for video understanding. In terms of data, we have obtained millions of annotated binary question-answering pairs. Initially, we performed a balanced sampling on each binary question by addressing the imbalance between positive and negative examples, ensuring a roughly equal number of positive and negative instances associated with each binary question. Then we use balanced instruction tuning dataset consisting of binary questions to fine-tune base VLM.

2.2. Interpretable Preference Learning

Preference Learning.

Based on a series of binary responses (yes or no), we use linear weighted summaries to predict human preferences. This is achieved by mapping yes and no to 1 and -1, respectively, and constructing a feature vector $\mathbf{X} = \{x^i\}$, where $i = 1, \dots, n$ and n represents the number of binary questions. We use a set of linear weights to obtain a score that accurately reflects human preferences, expressed as follows:

$$\text{score} = \mathbf{x}^T \mathbf{w} = x_1 w_1 + x_2 w_2 + \dots + x_n w_n. \quad (1)$$

In order to learn these parameters, we collect a dataset of human preferences $\mathcal{D} = \{(\mathbf{X}_i, \mathbf{X}_j)\}$, compute the feature difference for each pair, given by $\Delta \mathbf{X} = \mathbf{X}_i - \mathbf{X}_j$, and the corresponding label is assigned as $y = 1$ or $y = 0$ depending on the human preference.

We then perform regression using the logistic regression model based on $\Delta \mathbf{X}$. The predicted value (probability) is

given by:

$$\hat{y} = \sigma(\Delta \mathbf{x}^T \mathbf{w}) = \frac{1}{1 + e^{-\Delta \mathbf{x}^T \mathbf{w}}}. \quad (2)$$

The objective function to be minimized during training is defined as:

$$\text{Loss}(\mathbf{w}) = -\mathbb{E} \left[y \log(\sigma(\Delta \mathbf{x}^T \mathbf{w})) + (1 - y) \log(1 - \sigma(\Delta \mathbf{x}^T \mathbf{w})) \right]. \quad (3)$$

Through minimizing this objective function, we aim to find the optimal weights \mathbf{w} to predict preferences.

Multi-Dimensional Prediction. Since weights of binary questions are get, we can define score of every question by reward(q^i) = $w^i * x^i$, where w^i and x^i is the corresponding weight and feature result of question q^i . For every dimension, we can define the score of certain dimension d_k as reward $R(d_k)$, and $R(d_k) = \sum \text{reward}(q^i)$ where $q^i \in d_k$. It's clearly that the final reward is the sum of $R(d_k)$ from all dimensions.

After determining the weights for binary-response questions, we formulate the reward function for each question as:

$$\text{reward}(q^i) = w^i \cdot x^i \quad (4)$$

where w^i denotes the weight and x^i represents the corresponding feature value for question q^i . For each evaluation dimension d_k , we define its dimensional reward $R(d_k)$ as the summation of rewards from all constituent questions within that dimension:

$$R(d_k) = \sum_{q^i \in d_k} \text{reward}(q^i) \quad (5)$$

The total system reward is subsequently computed as the cumulative sum across all dimensions:

$$R_{\text{total}} = \sum_k R(d_k) \quad (6)$$

Upon completion of VisionReward training, the system can execute visual diagnosis and linear weighting through a two-phase framework to predict human preferences.

2.3. Multi-Dimensional Preference Optimization

By calculating dimension-specific scores through intra-dimensional weighting, VisionReward facilitates multi-dimensional preference optimization. To empirically validate the model's capacity, we leverage Direct Preference Optimization (DPO) for Diffusion Models in our experiments, where VisionReward generates multi-dimensional preference pairs to guide the optimization process while maintaining inter-dimensional balance.

Preliminary. Given a data distribution $q(x_0)$, Diffusion models [14, 37, 38] contains forward process and reverse process. Forward process $q(x_{1:T}|x_0)$ gradually add noise to the data x_0 and reverse process $p_\theta(x_{0:T})$ learns transitions to recover data. Training diffusion model can be performed by evidence lower bound [21, 39]:

$$L_{\text{DM}} = \mathbb{E}_{\mathbf{x}_0, \epsilon \sim \mathcal{N}(0, \mathbf{I}), t} \left[\|\epsilon - \epsilon_\theta(\mathbf{x}_t, t)\|_2^2 \right]. \quad (7)$$

with $t \sim \mathcal{U}(0, T)$ and $\mathbf{x}_t \sim q(\mathbf{x}_t | \mathbf{x}_0)$.

By learning to recover images, diffusion models are able to generate images that are meaningful to humans. However, just learning on recovering data can not learn to meet human's preference and needs. Some works have explored to use human preference to guide diffusion to move close to humans. Diffusion-DPO [43] introduces to use preference pairs towards direct preference learning. We denote the "winning" and "losing" samples as x_0^w, x_0^l , and the objective is as follows:

$$L(\theta) = -\mathbb{E}_{(\mathbf{x}_0^w, \mathbf{x}_0^l) \sim \mathcal{D}, t \sim \mathcal{U}(0, T), \mathbf{x}_t^w \sim q(\mathbf{x}_t^w | \mathbf{x}_0^w), \mathbf{x}_t^l \sim q(\mathbf{x}_t^l | \mathbf{x}_0^l)} \log \sigma(-\beta T \omega(\lambda_t) (\|\epsilon^w - \epsilon_\theta(\mathbf{x}_t^w, t)\|_2^2 - \|\epsilon^w - \epsilon_{\text{ref}}(\mathbf{x}_t^w, t)\|_2^2 - (\|\epsilon^l - \epsilon_\theta(\mathbf{x}_t^l, t)\|_2^2 - \|\epsilon^l - \epsilon_{\text{ref}}(\mathbf{x}_t^l, t)\|_2^2))) \quad (8)$$

where λ_t is the signal-to-noise ratio.

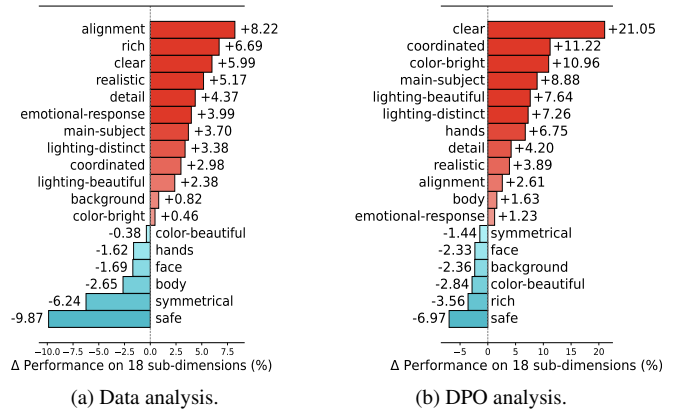


Figure 3. (a) We sample 10,000 human preference pairs from Pick-a-Pic [22] dataset and analyze score deviations across 18 sub-dimensions (represented by the average yes-proportion of checklist questions within each sub-dimension). (b) We compare score deviations for images generated by SDXL [31] before and after Diffusion-DPO fine-tuning [43], using the same 10,000 prompts.

Challenges. Although Diffusion-DPO has designed a direct preference optimization method to fine-tune text-to-image diffusion models, it suffers from being biased and over-optimized on certain dimensions such as aesthetic but gets somewhat worse, for example, less safe and more trouble about human body. We reproduce the procedure of

Diffusion-DPO and test the fine-tuned model on 10,000 sampled prompts from training data, using VisionReward to score images. Fig. 3 illustrates the changes across various dimensions after applying preference learning using the human preference dataset in which factors are coupled with different trade-offs.

MPO: Insight and Solution. We propose a multi-dimensional preference strategy (see Algorithm 1) to ensure comprehensive enhancement across all dimensions. Following Sec. 2.2, we obtain dimensional reward $R(d_k)$ and total reward R_{total} for each generated image. For two images x^i and x^j , we define R^i as dominating R^j if $R(d_k^i) \geq R(d_k^j)$ holds for every dimension d_k . The key differences between the MPO strategy and standard DPO are:

- **Standard DPO:** During DPO optimization, we generate m images per prompt and directly select the pair with the maximal difference in total reward R_{total} .
- **MPO-enhanced DPO:** MPO strategy introduces an additional constraint: we only select pairs x_0^i and x_0^j if R^i dominates R^j , then proceed with standard DPO.

We analyze the effects of MPO in Sec. 3.3. The MPO strategy can also be applied to other algorithms, which we leave for future exploration.

Algorithm 1 Multi-Dimensional Preference Optimization (MPO)

- 1: **Dataset:** Prompt set \mathcal{C} , question set for reward model $\mathcal{Q} = \{q_1, q_2, \dots, q_n\}$
 - 2: **Input:** Diffusion model p_θ , reward model r , the number of generate images per prompt m
 - 3: **Initialization:** Dominated set for MPO $\mathcal{D} \leftarrow \emptyset$
 - 4: **for** $c \in \mathcal{C}$ **do**
 - 5: Sample a set of images $\{x_0^1, x_0^2, \dots, x_0^m\} \sim p_\theta(x_0|c)$
 - 6: **for** $i = 1$ to m **do**
 - 7: Reward set $R_i \leftarrow \emptyset$
 - 8: **for** $j = 1$ to n **do**
 - 9: Add reward $r(q_j|x_0^i)$ to R_i
 - 10: **for** $i, j \sim \{1, 2, \dots, m\}$ **do**
 - 11: **if** R_i dominate R_j **then**
 - 12: Add $\{c, x_0^i, x_0^j\}$ to \mathcal{D}
 - 13: **for** $data \sim \mathcal{D}$ **do**
 - 14: Update the gradient p_θ from Eq. (8)
-

3. Experiments

3.1. VisionReward for Text-to-Vision Evaluation

Dataset & Training Setting. After balanced sampling, we obtain 40,743 images and corresponding training data containing 97,680 judgment questions from images, leaving 6,910 images for subsequent validation and test. For videos, we obtain 28,605 videos and corresponding training data containing 89,473 judgment questions, with 3,080 videos reserved.

To fine-tune CogVLM2 [18], we set a batch size of 64, a learning rate of 1e-6, and train for 1,500 steps. For

Type	Image	Video
Content	People, Objects, Animals, Architecture, Landscape, Vehicles, Plants, Food, Others, Scenes	Story, Human Activity, Artificial Scene, Others, Natural Animal Activity, Physical Phenomena
Challenge	Unreal, Style, History, Fine-grained Detail, Color, Famous Character, Normal, Famous Places, Writing, Complex Combo, Positional, Counting,	Material, Angle and Lens, Emotional Expression, Color/Tone, Surreal, World Knowledge, Special Effects, Text, Spatial Relationship, Camera Movement, Logical Consistency, Style, Temporal Speed

Table 1. Content and Challenge Categories of MonetBench.

CogVLM-Video, we set a batch size of 64, a learning rate of 4e-6, and train for 1,500 steps.

To learn linear weights for preference prediction, we sample human preference pairs and perform logistic regression. For images, We sample 44k pairs (24k from HPDv2 [47] and 20k from ImageRewardDB [49]); and for videos, we sample prompts from VidProM [44] and generate videos (using CogVideoX [50], VideoCrafter2 [4] and OpenSora [54]), getting 1,795 annotated video pairs with preference.

To establish a comprehensive evaluation benchmark for both image and video generation, we construct **MonetBench**, which contains separate test sets for images and videos, each consisting of 1,000 prompts. Tab. 1 shows content and challenge categories for MonetBench. More details are introduced in Appendix Sec. 11.

Main Results: Preference Accuracy. Preference accuracy means the probability that a reward model has the same judgment as humans about which image is better. We use MonetBench to construct our test set for human preference, using SDXL [31] to generate images and CogVideoX [50] / VideoCrafter2 [4] / OpenSora [54] to generate videos, resulting in 500 pairs for image and 1,000 pairs for video. We employ annotators to assess the generated images using a preference rating scale from 1 to 5 (with 3 indicating no preference). The average preference score is used as the final preference label. We also take HPDv2 [47] and GenAI-Bench [20] as test set.

Tab. 2 shows that VisionReward obtains state-of-the-state results in multiple datasets. Notably, in video evaluation, image reward models demonstrate competitive performance when the video duration is within 2 seconds (GenAI-Bench). However, when **the video duration reaches 6 seconds (MonetBench)**, only VisionReward is capable of accurately predicting human preference, being twice (**22.1% over random**) as high as the best (12.5% over random) among other methods. This indicates that dynamic information in longer videos poses a challenge for RMs, while

Method	Image				Video			
	HPDv2 [47]	MonetBench		GenAI-Bench [20]		MonetBench		
		tau*	diff**	tau	diff	tau	diff	
<i>task-specific discriminative models</i>								
ImageReward [49]	74.0	48.8	56.5	48.4	72.1	55.8	58.4	
PickScore [22]	79.8	49.8	57.6	<u>52.4</u>	<u>75.4</u>	57.7	61.6	
HPSv2 [47]	83.3	48.4	55.6	49.3	73.0	59.3	62.5	
MPS [52]	<u>83.5</u>	44.2	50.7	46.9	67.6	55.8	58.9	
<i>generative models</i>								
GPT-4o [1]	77.5	38.9	52.7	41.8	54.3	45.7	48.3	
Gemini [41]	60.7	27.4	55.1	46.9	61.7	52.2	56.8	
VQAScore [27]	69.7	49.4	56.5	45.2	68.0	56.1	59.5	
VideoScore [12]	76.8	45.8	52.5	47.8	71.4	49.1	54.9	
VisionReward (Ours)	81.7	51.8	59.5	51.8	74.4	64.0	72.1	

Table 2. Preference accuracy on multiple dataset. **Bold** denotes the best score within the generative models, while underline signifies the best score among all categories. Tau* means taking account of ties [8], and diff** means dropping ties in labels (we drop ties both in labels and responses for GPT-4o and Gemini in diff** because too many ties are given by them).

Method	Image				Video			
	Composition	Quality	Fidelity	Safety&Emotion	Stability	Dynamic	Physics	Preservation
LLaVa*	59.9	65.7	59.8	64.4	52.5	53.8	50.6	47.5
CogVLM2 [18]	65.8	67.1	53.1	74.7	49.3	57.1	51.2	47.8
GPT-4o [1]	73.1	62.7	61.9	70.1	57.9	69.1	62.4	58.8
Gemini [41]	69.4	59.9	59.7	74.9	58.1	71.1	58.1	59.6
VisionReward (Ours)	78.8	81.1	80.9	83.9	64.8	75.4	68.1	72.0

Table 3. Accuracy of VisionReward and other vision-language models (VLMs) on vision quality questions constructed from our annotation. *We test LLaVA-v1.5-7B [28] for image and LLava-Next-Video-34B [24] for video.

Composition	Quality	Fidelity	Safety
97.9	98.2	98.3	99.1
Stability	Dynamic	Physics	Preservation
97.4	99.9	88.2	99.8

Table 4. Consistency of VisionReward in each dimension.

VisionReward can effectively address this issue after fine-grained visual learning.

Main Results: Accuracy and Consistency on Judgment.

To evaluate the effectiveness of judgment learning, we construct a visual quality QA set to assess the visual assessment capabilities of VisionReward compared to other VLMs. We collect 1,364 test cases for images involving 14 types of questions across 4 dimensions, and additionally 1,308 cases covering 8 types of questions across 4 dimensions related to **dynamic content in videos**. To ensure the generality of these questions, we combine adjacent degrees in the checklists under each sub-dimension, enhancing distinctiveness and minimizing incidental subjectivity. Tab. 3 demon-

strates VisionReward’s superiority in judging visual quality over existing generalized multimodal LLMs, which remains a challenge for generalized multimodal LLMs.

As questions corresponding to each sub-dimension assess varying degrees of a particular factor, it’s important to measure consistency of VisionReward across multiple questions of the same sub-dimension. Consistency measures the likelihood that the model provides consistent responses across a series of judgments concerning this factor. Tab. 4 shows that VisionReward has high consistency (more than 97 %) in most (7 of 8) dimensions.

Ablation Study: Impact of Training Set Size. We conduct experiments with varying sizes of the training set to investigate its influence on regression performance. As demonstrated in Tab. 5, the accuracy improves monotonically as the training set size increases up to 4,000 samples, beyond which the accuracy stabilizes.

Ablation Study: Scalability of Question Scale. Tab. 6 shows that accuracy of preference prediction exhibits significant improvement as the question scale increases. Scal-

ability validates the effects of decomposing preferences via multi-scale questioning. We do more analysis such as question pruning in Appendix Sec. 8.

Size	200	500	1k	2k	4k	8k
Acc.	77.6	80.3	80.6	80.9	81.3	81.3

Table 5. Accuracy on HPDV2-test for different sizes of train set.

#question	2	4	8	16	32	all
Acc.	59.3	68.6	72.5	75.8	78.9	81.7

Table 6. Accuracy on HPDV2-test for different question scales.

3.2. VisionReward for Text-to-Vision Optimization

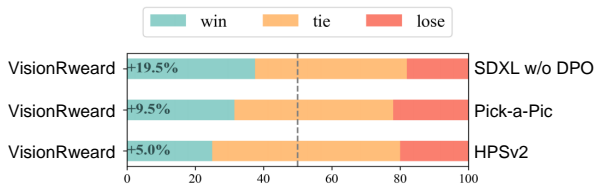


Figure 4. Human evaluation results of text-to-image DPO.

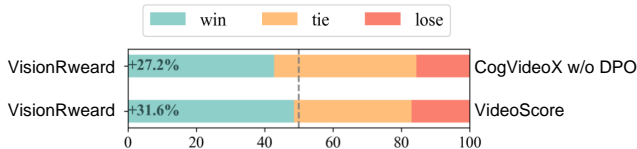


Figure 5. Human evaluation results of text-to-video DPO.

To evaluate the efficacy of VisionReward in preference optimization for visual generative systems, we conducted a series of comparative experiments against current state-of-the-art reward models and established preference datasets. The empirical results presented in Fig. 4 and Fig. 5 demonstrate VisionReward’s superior performance in both text-to-image and text-to-video optimization, achieving statistically significant improvements in human preference metrics over competing approaches.

This section focuses on preference optimization for text-to-video using different reward models. Details of text-to-image are provided in Appendix Sec. 9.2 due to page limits.

Dataset & Training Settings. For our backbone model, we select CogVideoX-2B¹. The training prompts are sampled from VidProM [44]. To adapt these prompts for video generation, we have optimized them following guidelines from CogVideoX [50], which results in roughly 22,000 samples. We generate 4 videos for each prompt, and use VisionReward to score these videos and apply the MPO strategy to

¹<https://huggingface.co/THUDM/CogVideoX-2b>

select approximately 9,400 effective preference pairs. In all our experiments, we maintain a batch size of 32, a learning rate of 5e-6, and employ 100 warmup steps followed by linear decay. We set the DPO parameter β to 500. The MPO training process spans around 500 steps, equivalent to about 2 epochs. During training, we save a checkpoint every 40 steps and use a validation set split from the training set to pick the checkpoint with the highest reward.

Evaluation Settings. To comprehensively assess the MPO models, we have conducted both automatic and human evaluations. The automatic evaluation is conducted across various benchmarks, including VBench [19] and our Video-MonetBench. For VBench, we focus on commonly reported key metrics, including *Human Action*, *Scene*, *Multiple Objects*, and *Appearance Style (Appear. Style)*. For human evaluation, annotators are asked to watch two videos and select the better one, with an option to indicate a tie if neither stands out. This manual assessment also uses the tasks in MonetBench. In all these experiments, we utilize prompt optimization recommended in CogVideoX. Our baseline comparisons include the original CogVideoX-2B and DPO with VideoScore.

Methods	Human Action	Scene	Multiple Objects	Appear. Style
Original	98.20	55.60	68.43	24.20
VideoScore	97.60	56.25	68.66	23.96
VisionReward	98.40	57.57	71.54	24.02

Table 7. Evaluation results on VBench.

Methods	Stability	Dynamic	Physics	Preservation
Original	0.272	0.047	0.323	0.584
VideoScore	0.242	0.046	0.319	0.557
VisionReward	0.309	0.036	0.337	0.661

Table 8. Evaluation results on MonetBench.

Experimental Results. The main results are shown in Tab. 7 and Tab. 8. When compared to the original CogVideoX-2B, optimization with VisionReward significantly enhances model performance across these benchmarks. In contrast, optimization with VideoScore tends to degrade performance. The empirical evidence substantiates VisionReward’s advanced capacity for multi-dimensional optimization. (Case study in Appendix Sec. 9.3.)

3.3. Effects of Multi-Dimensional Optimization

Ablation Study: Different Strategy for MPO. In using the MPO strategy, we define the way in which R^i dominates R^j (given two images x^i and x^j) to select pairs. The definition of “dominate” includes at least three methods for different reward objective: score of each dimension, score of each

sub-dimension, and score of each binary question. To investigate the impact of different definitions of “dominate”, we conduct experiments based on CogVideoX-5B. Specifically, we employ three different strategies, setting the threshold of the total score to 0.6, 0.5, and 0.4 respectively, ensuring that the number of pairs obtained through all three strategies is 5k. We use a batch size of 64, a learning rate of 2e-6, the DPO parameter β of 500, and the training steps of 300. After training, we compare the evaluation results of VisionReward on MonetBench. Tab. 9 shows that using the score for each dimension as objective yields the best results.

Methods	Baseline	Dimension	Sub-dimension	Question
Reward	4.303	4.573	4.539	4.514

Table 9. Score of VisionReward after different strategies of MPO. Dimension: “dominate” based on score of each dimension. Sub-dimension: “dominate” based on score of each sub-dimension. Question: “dominate” based on score of each binary question.

Method	Align.	Quality	Dynamic	Physics	Preserv.	Overall
Original	1.733	0.660	0.053	0.344	0.653	4.303
DPO	1.697	0.680	0.034	0.356	0.741	4.515
DPO w/ MPO	1.766	0.688	0.042	0.356	0.721	4.573
MaPO	1.736	0.660	0.052	0.345	0.645	4.295
MaPO w/ MPO	1.737	0.656	0.055	0.349	0.649	4.321

Table 10. Ablation Study for MPO strategy. Scores are given by VisionReward on MonetBench.

Ablation Study: Multi-Dimensional or Single Score. To comprehensively illustrate how MPO addresses the factor optimization bias inherent in DPO, we extend the previously described experimental setup by utilizing the total score of VisionReward to select pairs, setting the threshold at 0.8 to ensure consistency in numbers. VisionReward is employed to evaluate scores across various dimensions, with the detailed results presented in Tab. 10. Through the implementation of the MPO strategy, CogVideoX is optimized in such a manner that it avoids the degradation of certain factors (e.g., alignment), thereby achieving improved trade-offs, such as maintaining good preservation while avoiding excessively slow dynamic changes. The empirical evidence further substantiates VisionReward’s capacity for algorithm-agnostic preference alignment, as evidenced by comparative testing with other approaches like MaPO [16].

For efficiency discussion, the experimental results in Tab. 11 reveal the comparative effectiveness of the MPO and DPO methods. These results suggest that MPO outperforms the DPO approach in terms of both efficiency and effectiveness.

These findings highlight promising directions for future research in developing novel optimization algorithms and

adapting VisionReward for multi-dimensional optimization and preference balancing.

Method	Threshold	#Sample	Overall
DPO	0.6	6473	4.442
DPO	0.8	5270	4.515
MPO	0.6	5028	4.573

Table 11. More comparison of MPO and DPO on MonetBench.

4. Related Work

Evaluation for Text-to-image and Text-to-video. The development of multimodal generative models is advancing rapidly, including text-to-image [2, 9, 31, 33–35] and text-to-video [4, 15, 17, 42, 50, 54] models that generate high-quality images or videos based on given textual input. For text-to-image, early evaluations heavily relied on metrics such as FID [13] and CLIP [32] Score. Recent work [49] has pointed out that these metrics may not align well with human preferences. Many metrics based on reward models learn from human preferences [22, 47, 49], resulting in a single score, which can lead to biases. With the advancement of Vision-Language Models (VLMs) [1, 18, 24, 28, 41, 45], some studies [27, 53] have attempted to directly use VLMs to assess images, considering aspects like alignment and quality. Nevertheless, we find that VLMs have a gap in their ability to accurately assess vision quality. VisionReward proposes a fine-grained, multi-dimensional evaluation framework, using specialized judgment instructions to achieve more accurate and interpretable.

RLHF for Text-to-image and Text-to-video. Reinforcement Learning from Human Feedback (RLHF) [29, 30, 40] refers to optimizing models with reinforcement learning based on human feedback, which has been proven to significantly enhance language models. For visual generation tasks, several works have explored RLHF, optimizing from the gradient [48, 49] or using a policy-based RL approach [3, 7, 10]. All these methods require a reward model (RM) to provide feedback for online learning. Diffusion-DPO [43] has proposed to optimize the diffusion model directly using human-labeled preference data. However, most RLHF methods face the issue of over-optimization. VisionReward highlights that these issues are because of excessive optimization of some factors and degradation of others. By employing a Pareto-optimality approach from a multi-objective perspective, VisionReward achieves robust RLHF.

5. Conclusion

We introduce VisionReward, a reward model for visual generation, which is fine-grained and multi-dimensional. By enabling Vision-Language Model (VLM) to perform binary

assessments and applying linear summation with weighting coefficients derived from preference learning, VisionReward achieves highly accurate and interpretable. For visual generative optimization, VisionReward surpasses other reward models and enable multi-dimensional strategy.

6. Acknowledgments

The authors would like to thank Zhipu AI for sponsoring the computation resources used in this work.

References

- [1] Josh Achiam, Steven Adler, Sandhini Agarwal, Lama Ahmad, Ilge Akkaya, Florencia Leoni Aleman, Diogo Almeida, Janko Altenschmidt, Sam Altman, Shyamal Anadkat, et al. Gpt-4 technical report. *arXiv preprint arXiv:2303.08774*, 2023. 1, 6, 8
- [2] James Betker, Gabriel Goh, Li Jing, Tim Brooks, Jianfeng Wang, Linjie Li, Long Ouyang, Juntang Zhuang, Joyce Lee, Yufei Guo, et al. Improving image generation with better captions. *Computer Science*. <https://cdn.openai.com/papers/dall-e-3.pdf>, 2(3):8, 2023. 1, 8
- [3] Kevin Black, Michael Janner, Yilun Du, Ilya Kostrikov, and Sergey Levine. Training diffusion models with reinforcement learning. *arXiv preprint arXiv:2305.13301*, 2023. 1, 8
- [4] Haoxin Chen, Yong Zhang, Xiaodong Cun, Menghan Xia, Xintao Wang, Chao Weng, and Ying Shan. Videocrafter2: Overcoming data limitations for high-quality video diffusion models. In *Proceedings of the IEEE/CVF Conference on Computer Vision and Pattern Recognition*, pages 7310–7320, 2024. 1, 5, 8, 12
- [5] Tsai-Shien Chen, Aliaksandr Siarohin, Willi Menapace, Ekaterina Deyneka, Hsiang-wei Chao, Byung Eun Jeon, Yuwei Fang, Hsin-Ying Lee, Jian Ren, Ming-Hsuan Yang, et al. Panda-70m: Captioning 70m videos with multiple cross-modality teachers. In *Proceedings of the IEEE/CVF Conference on Computer Vision and Pattern Recognition*, pages 13320–13331, 2024. 12
- [6] Zhaorun Chen, Yichao Du, Zichen Wen, Yiyang Zhou, Chenhang Cui, Zhenzhen Weng, Haoqin Tu, Chaoqi Wang, Zhengwei Tong, Qinglan Huang, et al. Mj-bench: Is your multimodal reward model really a good judge for text-to-image generation? *arXiv preprint arXiv:2407.04842*, 2024. 1
- [7] Kevin Clark, Paul Vicol, Kevin Swersky, and David J Fleet. Directly fine-tuning diffusion models on differentiable rewards. *arXiv preprint arXiv:2309.17400*, 2023. 1, 8
- [8] Daniel Deutsch, George Foster, and Markus Freitag. Ties matter: Meta-evaluating modern metrics with pairwise accuracy and tie calibration. In *Proceedings of the 2023 Conference on Empirical Methods in Natural Language Processing*, pages 12914–12929, 2023. 6
- [9] Ming Ding, Zhuoyi Yang, Wenyi Hong, Wendi Zheng, Chang Zhou, Da Yin, Junyang Lin, Xu Zou, Zhou Shao, Hongxia Yang, et al. Cogview: Mastering text-to-image generation via transformers. *Advances in Neural Information Processing Systems*, 34:19822–19835, 2021. 1, 8
- [10] Ying Fan, Olivia Watkins, Yuqing Du, Hao Liu, Moonkyung Ryu, Craig Boutilier, Pieter Abbeel, Mohammad Ghavamzadeh, Kangwook Lee, and Kimin Lee. Dpoc: reinforcement learning for fine-tuning text-to-image diffusion models. In *Proceedings of the 37th International Conference on Neural Information Processing Systems*, pages 79858–79885, 2023. 1, 8
- [11] Team GLM, :, Aohan Zeng, Bin Xu, Bowen Wang, Chenhui Zhang, Da Yin, Dan Zhang, Diego Rojas, Guanyu Feng, Hanlin Zhao, Hanyu Lai, Hao Yu, Hongning Wang, Jiadai Sun, Jiajie Zhang, Jiale Cheng, Jiayi Gui, Jie Tang, Jing Zhang, Jingyu Sun, Juanzi Li, Lei Zhao, Lindong Wu, Lucen Zhong, Mingdao Liu, Minlie Huang, Peng Zhang, Qinkai Zheng, Rui Lu, Shuaiqi Duan, Shudan Zhang, Shulin Cao, Shuxun Yang, Weng Lam Tam, Wenyi Zhao, Xiao Liu, Xiao Xia, Xiaohan Zhang, Xiaotao Gu, Xin Lv, Xinghan Liu, Xinyi Liu, Xinyue Yang, Xixuan Song, Xunkai Zhang, Yifan An, Yifan Xu, Yilin Niu, Yuantao Yang, Yueyan Li, Yushi Bai, Yuxiao Dong, Zehan Qi, Zhaoyu Wang, Zhen Yang, Zhengxiao Du, Zhenyu Hou, and Zihan Wang. Chatglm: A family of large language models from glm-130b to glm-4 all tools, 2024. 12, 28
- [12] Xuan He, Dongfu Jiang, Ge Zhang, Max Ku, Achint Soni, Sherman Siu, Haonan Chen, Abhrranil Chandra, Ziyang Jiang, Aaran Arulraj, et al. Videoscore: Building automatic metrics to simulate fine-grained human feedback for video generation. In *Proceedings of the 2024 Conference on Empirical Methods in Natural Language Processing*, pages 2105–2123, 2024. 1, 2, 6
- [13] Martin Heusel, Hubert Ramsauer, Thomas Unterthiner, Bernhard Nessler, and Sepp Hochreiter. Gans trained by a two time-scale update rule converge to a local nash equilibrium. *Advances in neural information processing systems*, 30, 2017. 8
- [14] Jonathan Ho, Ajay Jain, and Pieter Abbeel. Denoising diffusion probabilistic models. *Advances in neural information processing systems*, 33:6840–6851, 2020. 4
- [15] Jonathan Ho, William Chan, Chitwan Saharia, Jay Whang, Ruiqi Gao, Alexey Gritsenko, Diederik P Kingma, Ben Poole, Mohammad Norouzi, David J Fleet, et al. Imagen video: High definition video generation with diffusion models. *arXiv preprint arXiv:2210.02303*, 2022. 1, 8
- [16] Jiwoo Hong, Sayak Paul, Noah Lee, Kashif Rasul, James Thorne, and Jongheon Jeong. Margin-aware preference optimization for aligning diffusion models without reference. *arXiv preprint arXiv:2406.06424*, 2024. 8
- [17] Wenyi Hong, Ming Ding, Wendi Zheng, Xinghan Liu, and Jie Tang. Cogvideo: Large-scale pretraining for text-to-video generation via transformers. *arXiv preprint arXiv:2205.15868*, 2022. 1, 8
- [18] Wenyi Hong, Weihang Wang, Ming Ding, Wenmeng Yu, Qingsong Lv, Yan Wang, Yean Cheng, Shiyu Huang, Junhui Ji, Zhao Xue, et al. Cogvlm2: Visual language models for image and video understanding. *arXiv preprint arXiv:2408.16500*, 2024. 3, 5, 6, 8

- [19] Ziqi Huang, Yinan He, Jiashuo Yu, Fan Zhang, Chenyang Si, Yuming Jiang, Yuanhan Zhang, Tianxing Wu, Qingyang Jin, Nattapol Chanpaisit, et al. Vbench: Comprehensive benchmark suite for video generative models. In *Proceedings of the IEEE/CVF Conference on Computer Vision and Pattern Recognition*, pages 21807–21818, 2024. 7
- [20] Dongfu Jiang, Max Ku, Tianle Li, Yuansheng Ni, Shizhuo Sun, Rongqi Fan, and Wenhui Chen. Genai arena: An open evaluation platform for generative models. *arXiv preprint arXiv:2406.04485*, 2024. 5, 6
- [21] Diederik Kingma, Tim Salimans, Ben Poole, and Jonathan Ho. Variational diffusion models. *Advances in neural information processing systems*, 34:21696–21707, 2021. 4
- [22] Yuval Kirstain, Adam Polyak, Uriel Singer, Shahbuland Matiana, Joe Penna, and Omer Levy. Pick-a-pic: An open dataset of user preferences for text-to-image generation. *Advances in Neural Information Processing Systems*, 36:36652–36663, 2023. 1, 4, 6, 8, 12, 28
- [23] Chunyi Li, Zicheng Zhang, Haoning Wu, Wei Sun, Xionghuo Min, Xiaohong Liu, Guangtao Zhai, and Weisi Lin. Agiqa-3k: An open database for ai-generated image quality assessment. *IEEE Transactions on Circuits and Systems for Video Technology*, 34(8):6833–6846, 2023. 1
- [24] Feng Li, Renrui Zhang, Hao Zhang, Yuanhan Zhang, Bo Li, Wei Li, Zejun Ma, and Chunyuan Li. Llava-next-interleave: Tackling multi-image, video, and 3d in large multimodal models. *arXiv preprint arXiv:2407.07895*, 2024. 6, 8
- [25] Youwei Liang, Junfeng He, Gang Li, Peizhao Li, Arseniy Klimovskiy, Nicholas Carolan, Jiao Sun, Jordi Pont-Tuset, Sarah Young, Feng Yang, et al. Rich human feedback for text-to-image generation. In *Proceedings of the IEEE/CVF Conference on Computer Vision and Pattern Recognition*, pages 19401–19411, 2024. 2
- [26] Chin-Yew Lin. ROUGE: A package for automatic evaluation of summaries. In *Text Summarization Branches Out*, pages 74–81, Barcelona, Spain, 2004. Association for Computational Linguistics. 28
- [27] Zhiqiu Lin, Deepak Pathak, Baiqi Li, Jiayao Li, Xide Xia, Graham Neubig, Pengchuan Zhang, and Deva Ramanan. Evaluating text-to-visual generation with image-to-text generation. In *European Conference on Computer Vision*, pages 366–384. Springer, 2025. 6, 8, 14
- [28] Haotian Liu, Chunyuan Li, Qingyang Wu, and Yong Jae Lee. Visual instruction tuning, 2023. 6, 8
- [29] Reiichiro Nakano, Jacob Hilton, Suchir Balaji, Jeff Wu, Long Ouyang, Christina Kim, Christopher Hesse, Shantanu Jain, Vineet Kosaraju, William Saunders, et al. Webgpt: Browser-assisted question-answering with human feedback. *arXiv preprint arXiv:2112.09332*, 2021. 8
- [30] Long Ouyang, Jeffrey Wu, Xu Jiang, Diogo Almeida, Carroll Wainwright, Pamela Mishkin, Chong Zhang, Sandhini Agarwal, Katarina Slama, Alex Ray, et al. Training language models to follow instructions with human feedback. *Advances in Neural Information Processing Systems*, 35:27730–27744, 2022. 1, 8
- [31] Dustin Podell, Zion English, Kyle Lacey, Andreas Blattmann, Tim Dockhorn, Jonas Müller, Joe Penna, and Robin Rombach. Sdxl: Improving latent diffusion models for high-resolution image synthesis. *arXiv preprint arXiv:2307.01952*, 2023. 1, 4, 5, 8
- [32] Alec Radford, Jong Wook Kim, Chris Hallacy, Aditya Ramesh, Gabriel Goh, Sandhini Agarwal, Girish Sastry, Amanda Askell, Pamela Mishkin, Jack Clark, et al. Learning transferable visual models from natural language supervision. In *International conference on machine learning*, pages 8748–8763. PMLR, 2021. 8, 14
- [33] Aditya Ramesh, Mikhail Pavlov, Gabriel Goh, Scott Gray, Chelsea Voss, Alec Radford, Mark Chen, and Ilya Sutskever. Zero-shot text-to-image generation. In *International conference on machine learning*, pages 8821–8831. Pmlr, 2021. 1, 8
- [34] Robin Rombach, Andreas Blattmann, Dominik Lorenz, Patrick Esser, and Bjorn Ommer. High-resolution image synthesis with latent diffusion models. In *2022 IEEE/CVF Conference on Computer Vision and Pattern Recognition (CVPR)*, pages 10674–10685. IEEE Computer Society, 2022.
- [35] Chitwan Saharia, William Chan, Saurabh Saxena, Lala Li, Jay Whang, Emily L Denton, Kamyar Ghasemipour, Raphael Gontijo Lopes, Burcu Karagol Ayan, Tim Salimans, et al. Photorealistic text-to-image diffusion models with deep language understanding. *Advances in neural information processing systems*, 35:36479–36494, 2022. 1, 8, 14
- [36] Christoph Schuhmann, Romain Beaumont, Richard Vencu, Cade W Gordon, Ross Wightman, Mehdi Cherti, Theo Coombes, Aarush Katta, Clayton Mullis, Mitchell Wortsman, et al. Laion-5b: An open large-scale dataset for training next generation image-text models. In *Thirty-sixth Conference on Neural Information Processing Systems Datasets and Benchmarks Track*, 2022. 14
- [37] Jascha Sohl-Dickstein, Eric Weiss, Niru Maheswaranathan, and Surya Ganguli. Deep unsupervised learning using nonequilibrium thermodynamics. In *International conference on machine learning*, pages 2256–2265. PMLR, 2015. 4
- [38] Yang Song, Jascha Sohl-Dickstein, Diederik P Kingma, Abhishek Kumar, Stefano Ermon, and Ben Poole. Score-based generative modeling through stochastic differential equations. *arXiv preprint arXiv:2011.13456*, 2020. 4
- [39] Yang Song, Conor Durkan, Iain Murray, and Stefano Ermon. Maximum likelihood training of score-based diffusion models. *Advances in neural information processing systems*, 34:1415–1428, 2021. 4
- [40] Nisan Stiennon, Long Ouyang, Jeffrey Wu, Daniel Ziegler, Ryan Lowe, Chelsea Voss, Alec Radford, Dario Amodei, and Paul F Christiano. Learning to summarize with human feedback. *Advances in Neural Information Processing Systems*, 33:3008–3021, 2020. 8
- [41] Gemini Team, Petko Georgiev, Ving Ian Lei, Ryan Burnell, Libin Bai, Anmol Gulati, Garrett Tanzer, Damien Vincent, Zhufeng Pan, Shibo Wang, et al. Gemini 1.5: Unlocking multimodal understanding across millions of tokens of context. *arXiv preprint arXiv:2403.05530*, 2024. 1, 6, 8
- [42] Ruben Villegas, Mohammad Babaeizadeh, Pieter-Jan Kinndermans, Hernan Moraldo, Han Zhang, Mohammad Taghi

- Saffar, Santiago Castro, Julius Kunze, and Dumitru Erhan. Phenaki: Variable length video generation from open domain textual descriptions. In *International Conference on Learning Representations*, 2022. 1, 8
- [43] Bram Wallace, Meihua Dang, Rafael Rafailov, Linqi Zhou, Aaron Lou, Senthil Purushwalkam, Stefano Ermon, Caiming Xiong, Shafiq Joty, and Nikhil Naik. Diffusion model alignment using direct preference optimization. In *Proceedings of the IEEE/CVF Conference on Computer Vision and Pattern Recognition*, pages 8228–8238, 2024. 2, 4, 8, 15
- [44] Wenhao Wang and Yi Yang. Vidprom: A million-scale real prompt-gallery dataset for text-to-video diffusion models. *arXiv preprint arXiv:2403.06098*, 2024. 5, 7, 28
- [45] Weihao Wang, Qingsong Lv, Wenmeng Yu, Wenyi Hong, Ji Qi, Yan Wang, Junhui Ji, Zhuoyi Yang, Lei Zhao, Xixuan Song, et al. Cogvlm: Visual expert for pretrained language models. *arXiv preprint arXiv:2311.03079*, 2023. 8
- [46] Hao Wu, Jiayuan Mao, Yufeng Zhang, Yuning Jiang, Lei Li, Weiwei Sun, and Wei-Ying Ma. Unified visual-semantic embeddings: Bridging vision and language with structured meaning representations. In *2019 IEEE/CVF Conference on Computer Vision and Pattern Recognition (CVPR)*, pages 6602–6611, 2019. 14
- [47] Xiaoshi Wu, Yiming Hao, Keqiang Sun, Yixiong Chen, Feng Zhu, Rui Zhao, and Hongsheng Li. Human preference score v2: A solid benchmark for evaluating human preferences of text-to-image synthesis. *arXiv preprint arXiv:2306.09341*, 2023. 1, 5, 6, 8, 12
- [48] Xiaoshi Wu, Yiming Hao, Manyuan Zhang, Keqiang Sun, Zhaoyang Huang, Guanglu Song, Yu Liu, and Hongsheng Li. Deep reward supervisions for tuning text-to-image diffusion models. *arXiv preprint arXiv:2405.00760*, 2024. 8
- [49] Jiazhen Xu, Xiao Liu, Yuchen Wu, Yuxuan Tong, Qinkai Li, Ming Ding, Jie Tang, and Yuxiao Dong. Imagereward: learning and evaluating human preferences for text-to-image generation. In *Proceedings of the 37th International Conference on Neural Information Processing Systems*, pages 15903–15935, 2023. 1, 5, 6, 8, 12, 28
- [50] Zhuoyi Yang, Jiayan Teng, Wendi Zheng, Ming Ding, Shiyu Huang, Jiazhen Xu, Yuanming Yang, Wenyi Hong, Xiaohan Zhang, Guanyu Feng, et al. Cogvideox: Text-to-video diffusion models with an expert transformer. *arXiv preprint arXiv:2408.06072*, 2024. 1, 5, 7, 8, 12
- [51] Jiacheng Zhang, Jie Wu, Yuxi Ren, Xin Xia, Huafeng Kuang, Pan Xie, Jiashi Li, Xuefeng Xiao, Min Zheng, Lean Fu, and Guanbin Li. Unifl: Improve stable diffusion via unified feedback learning, 2024. 14
- [52] Sixian Zhang, Bohan Wang, Junqiang Wu, Yan Li, Tingting Gao, Di Zhang, and Zhongyuan Wang. Learning multi-dimensional human preference for text-to-image generation. In *Proceedings of the IEEE/CVF Conference on Computer Vision and Pattern Recognition*, pages 8018–8027, 2024. 2, 6
- [53] Xinlu Zhang, Yujie Lu, Weizhi Wang, An Yan, Jun Yan, Lianke Qin, Heng Wang, Xifeng Yan, William Yang Wang, and Linda Ruth Petzold. Gpt-4v (ision) as a generalist evaluator for vision-language tasks. *arXiv preprint arXiv:2311.01361*, 2023. 8
- [54] Zangwei Zheng, Xiangyu Peng, Tianji Yang, Chenhui Shen, Shenggui Li, Hongxin Liu, Yukun Zhou, Tianyi Li, and Yang You. Open-sora: Democratizing efficient video production for all, 2024. 1, 5, 8, 12

VisionReward: Fine-Grained Multi-Dimensional Human Preference Learning for Image and Video Generation

Appendix

7. Details of Annotation and Dataset

7.1. Details of Annotation Pipeline

Details of Data Preparation. To ensure the diversity of our annotation, we collect our annotated data from various sources, as presented in Tab. 12. For images, we select 3 popular datasets: ImageRewardDB [49], HPDv2 [47], and Pick-a-Pic [22]. We sample 16k images from each dataset for annotation (with the first two sampling 4k prompts each associated with 4 images, and Pick-a-Pic sampling 8k prompts each associated with 2 images), totaling 48k annotated images. For videos, we conduct random sampling from the VidProM dataset and use ChatGLM [11] for data cleaning (prompt Cf. Tab. 13), leading to 10k prompts. Then we use CogVideoX [50], VideoCrafter2 [4] and OpenSora [54] to generate 30k videos, sample from Panda-70M [5] to get 3k real videos, leading to 33k videos for annotation.

Type	Source	#Samples	#Checklist
Image	ImageRewardDB [49]	16K	1M
	Pick-a-Pic [22]	16K	1M
	HPDv2 [47]	16K	1M
Video	CogVideoX [50]	10K	0.6M
	Open-Sora [54]	10K	0.6M
	VideoCrafter2 [4]	10K	0.6M
	Panda-70M [5]	3K	0.2M

Table 12. Statistics of source data and annotation.

Annotation Design. In the annotation process, we design a comprehensive dimensional system and divide each dimension into several sub-dimensions. Tab. 14 illustrates our preference dimensions and the checklist count. We identify 5 dimensions for text-to-image generation and expand to 9 dimensions for text-to-video. For each sub-dimension, we set options that vary gradually in degree. Annotators are required to label each sub-dimension for every image. In our annotation process, we design multiple-choice questions for each dimension, allowing annotators to select the option that best fits the image. Additionally, we further decompose these options into several binary (yes/no) questions, ultimately forming a checklist for evaluating each image or video. This checklist is then utilized for subsequent evaluation systems and reward model training.

Annotation Management. To avoid annotation bias of an-

notators, our approach includes:

- **Professional management.** Cooperated with a specialized company, we strictly conduct trial annotation training for the annotators, screen qualified annotators, and conduct secondary quality inspection of the annotation results.
- **Standard document.** Our annotation document gives clear definitions and provides more than 10 examples for each judgment, to align the standard among annotators.
- **Consistency test.** Consistency of annotators on checklist results in **89.29%** (images) and **89.33%** (videos).

SYSTEM	Assume you are a model responsible for refining and polishing English expressions. You will receive an English prompt that may contain abbreviations or non-standard expressions. Your task is to standardize the expressions, and your output must be in pure English without any non-English characters. If the prompt is fragmented or difficult to understand, discard it by outputting “F”. Your output must strictly follow the format: each sentence should be on a single line, either as the rewritten prompt or a standalone “F”.
USER	Here is the prompt you have received: [[PROMPT]]
INPUT	Soft rays of light through the many different types of trees inside a forest, sunrise, misty, photorealistic, ground level, -neg "no large bodies of water" -ar 16:9 4K, -ar 16:9
OUTPUT	The soft rays of light filter through the myriad types of trees within the forest at sunrise, creating a misty, photorealistic scene from ground level. Exclude any large bodies of water. The aspect ratio should be 16:9 in 4K resolution. Aspect ratio: 16:9.

Table 13. Prompt template and example for prompt cleaning.

7.2. Statistics of Annotation Result

Fig. 6 is the statistical results of the labeled data for images and videos. When compiling the statistics, higher

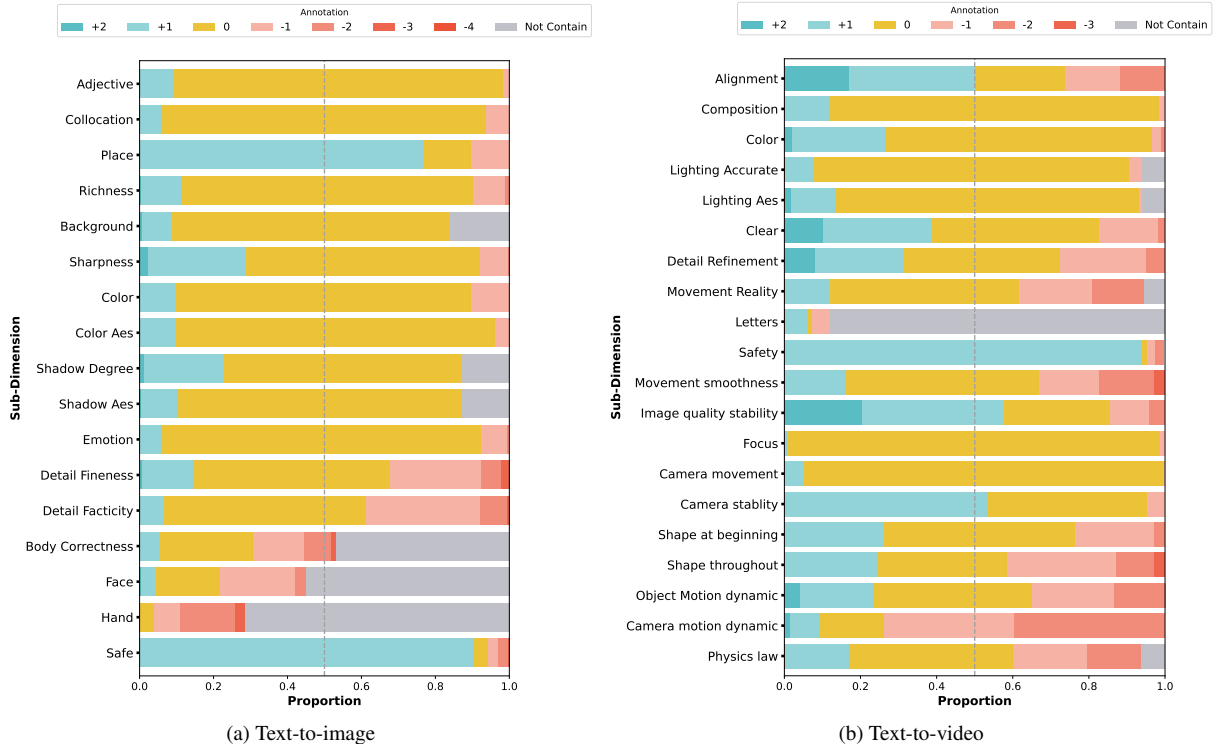


Figure 6. Annotation statistics of different sub-dimensions.

Dimension	#Sub-dimension		#Checklist	
	Image	Video	Image	Video
Alignment	1	1	1	4
Composition	5	1	13	2
Quality	5	4	14	14
Fidelity	5	3	25	9
Safety&Emotion	2	1	8	4
Stability	-	5	-	12
Dynamic	-	2	-	8
Physics	-	1	-	4
Preservation	-	2	-	7
Total	18	20	61	64

Table 14. Taxonomy of annotation for VisionReward.

labels indicate better performance for the image or video sub-dimension, while a label of 0 indicates neutrality. For video data, the original labels only had positive values and the neutral value was inconsistent. Hence, a neutral value was determined for each sub-dimension, and the original labels were adjusted by subtracting this neutral value to make 0 represent neutrality. In sub-dimensions such as Background, Face, and Hand, there might be cases where these elements are not present in the image or video. In such instances, "Not Contain" is treated as a separate category for

statistical purposes.

There are two main characteristics to note.

- For most sub-dimensions, the distribution of options roughly follows a normal distribution, with the majority being ordinary, and the quantities of instances with extreme characteristics, either very good or very bad, are reduced. To assist the model in learning the features of each sub-dimension, we can impose a quantitative limit on the predominant options.
- Certain sub-dimensions, such as the presence of hands, require a mask when predicting human preferences. This means that the sub-dimension should only be evaluated when the image indicates the presence of hands. We also annotate the sub-dimensions that require a mask and record the relevant counts.

8. More Details and Results of VisionReward

VisionReward comprises two steps: visual judgment and linear regression.

Visual Judgment Process. As the options for each sub-dimension are progressive, for any given option corresponding to a judgment question in the checklist, samples with an option greater than or equal to the given one are considered positive examples for the judgment question, whereas samples with an option less than the given one are considered

negative. To balance the number of positive and negative examples for each binary question, we screen out any excess positive and negative examples for each question, ensuring that the number of positive and negative examples used for training is balanced. For alignment, we use different methods on images and videos. For images, we use VQAScore [27] as an alignment judgment. For videos, we train five levels of judgment for VisionReward.

Weight Masking. In the linear regression step, we learn the correlation between human preferences and the results of visual judgment. In our design, if the result of the visual judgment is “yes”, human preference improves. We examine the correlation between human preference and each judgment result, and the numerical results indicate a positive correlation. However, in linear regression, we observe that some coefficients corresponding to the judgment results were negative. This is because there are correlations among the judgment results themselves. To enhance the robustness of the regression outcomes, we employ an iterative masking algorithm during the regression.

Algorithm 2 Iterative Regression with Weight Masking

Input: Dataset of human preferences $\mathcal{D} = \{(\mathbf{X}_i, \mathbf{X}_j, y)\}$, where each pair $(\mathbf{X}_i, \mathbf{X}_j)$ represents feature vectors of binary responses and $y \in \{0, 1\}$ is the human preference label

- 1: **Initialization:** Initialize linear weights $\mathbf{w} = [w_1, \dots, w_n]$
- 2: Initialize convergence criterion $\text{diff} \leftarrow \infty$
- 3: **while** $\text{diff} > \epsilon$ **do**
- 4: $\mathbf{w}_{\text{old}} \leftarrow \mathbf{w}$
- 5: **for each** $(\mathbf{X}_i, \mathbf{X}_j, y)$ **in** \mathcal{D} **do**
- 6: $\Delta \mathbf{X} \leftarrow \mathbf{X}_i - \mathbf{X}_j$
- 7: $\hat{y} \leftarrow \sigma(\Delta \mathbf{X}^T \mathbf{w})$
- 8: $\nabla_{\mathbf{w}} \text{Loss} = (\hat{y} - y) \Delta \mathbf{X}$
- 9: $\mathbf{w} \leftarrow \mathbf{w} - \alpha \nabla_{\mathbf{w}} \text{Loss}$
- 10: Mask negative weights $\mathbf{w} \leftarrow \mathbf{w} \odot (\mathbf{w} > 0)$
- 11: $\text{diff} \leftarrow \|\mathbf{w} - \mathbf{w}_{\text{old}}\|$

Output: Trained weights \mathbf{w}

Ablation Study: Efficiency of VisionReward via Weight Masking. We explore whether selective question pruning through coefficient thresholding could maintain model efficacy. As demonstrated in Tab. 15, coefficient-guided masking strategy (Acc. w/ mask) achieves remarkable efficiency gains with comparable accuracy.

#question	2	4	8	16	32	all
Acc. w/ mask	71.1	78.9	80.7	81.4	81.6	81.7

Table 15. Accuracy on HPDv2-test for different question scales. “Acc. w/ mask” means selecting questions by coefficient magnitude after full-set regression.

9. More Details and Results of MPO

9.1. Details of Prompt for MPO

Prompt Filtering. We employ the prompt filtering approach proposed by Zhang et al. [51] to curate our dataset. This strategy comprises two pivotal steps:

- **Semantic-Based Filtering:** Utilizing an existing scene graph parser [46], we evaluate the semantic richness of prompts by analyzing the number of subjective and objective relationships. Prompts with fewer than one meaningful relationship are filtered out to reduce noise data.
- **Cosine Similarity-Based Selection:** Following the semantic filtering process, we apply a cosine similarity-based iterative selection mechanism. By maintaining a maximum similarity threshold of 0.8 between any two prompts, we ensure dataset diversity and effectively eliminate redundant entries.

Dataset Curation. We apply this filtering strategy to the combined training sets from the Pick-a-Pick and HPS datasets, which initially comprise 166,475 prompts. Following comprehensive filtering, we retain 63,165 high-quality prompts for subsequent Multiobjective Preference Optimization (MPO) training.

9.2. VisionReward for Text-to-Image Optimization

Dataset & Training Settings. We strategically sample 63,165 prompts from existing datasets and generate 8 images per prompt using SDXL (this procedure theoretically produces 1.76M text-image pairs). Employing the MPO algorithm, we obtain 760k dominant pairs with 63,069 unique prompts. For comparison, we use HPSv2 with a threshold of 0.0015, getting 770k pairs with 63,107 unique prompts from the same source. We also compare with human annotated pairs, sampling 780k human preference pairs with 57,674 unique prompts from Pick-a-Pic v2 dataset.

We maintain consistent training parameters and dataset sizes across all experiments to ensure fair comparison. For all three experiments, we used an effective batch size of 256 (with GAS set to 4 and train batch size set to 1), set β to 5000, and a learning rate of 5e-9 (before scaling). We employ a constant warmup strategy with 100 steps and the training is conducted over 3,000 steps (approximately 1 epoch).

Evaluation Settings. We conducted both automatic and human evaluation on DrawBench [35]. Automatic evaluation includes multiple metrics such as human preference RMs, CLIP [32] and LAION-Aesthetic [36]. Human evaluation requires annotators to comprehensively evaluate two images and select the better one, with an option to indicate a tie if neither is preferred. Annotators are required to take different perspectives (such as composition, image quality, realism, safety, and image-text alignment) into account.

Experimental Results. Main results are demonstrated in Tab. 16 and Tab. 17. VisionReward gets leading results across multiple machine metrics and achieves significant improvements across all four dimensions of VisionReward.

Methods	CLIP	Aes	HPSv2	PickScore
Original	0.273	5.463	0.282	22.25
Pick-a-Pic	0.279	5.511	0.286	22.45
HPSv2	0.277	5.599	0.292	22.58
VisionReward	0.279	5.612	0.289	22.61

Table 16. Evaluation results of multiple metrics on DrawBench.

Methods	Composition	Quality	Fidelity	Safety
Original	0.755	0.550	0.009	-0.008
Pick-a-Pic	0.765	0.588	0.009	-0.009
HPSv2	0.874	0.630	0.010	-0.004
VisionReward	0.894	0.670	0.017	-0.001

Table 17. Evaluation results on MonetBench.

9.3. More Results of MPO

Case Study. Fig. 7 shows MPO cases for text-to-image, while Fig. 8 and Fig. 9 show MPO cases for text-to-video. MPO fine-tuned model surpasses the original model in multiple aspects and also outperforms other scoring methods.

Training Curve. Fig. 10 shows the variation of the dimensional scores during the MPO process with respect to the number of training samples. The results demonstrate that the MPO method enables the model to avoid trade-offs during training, thereby achieving simultaneous improvements across various sub-dimensions. In contrast, the DPO [43] method fails to achieve this level of concurrent enhancement.

10. Details of Dimensions for Annotation

Tab. 18 and Tab. 19 show the annotation taxonomy of images, while Tab. 20 and Tab. 21 show for videos.

Weight and Accuracy of Checklist. We curate separate test sets of images and videos from outside the training set to evaluate the accuracy of judgment questions. The test set comprises 1,209 images and 1,000 videos, respectively. We report the accuracy of judgment questions (Cf. Tab. 22 and Tab. 23 for text-to-image, Tab. 24 and Tab. 25 for text-to-video). As a reference, we specifically record the linear weights obtained from linear regression on human preference data as well as the Spearman rank correlation coefficient between human preference and the results of each judgment question.

Correlation of Sub Dimensions. To mine the correlation between the sub-dimensions after preference decou-

pling, we show the correlation coefficients between the sub-dimensions in a heat map (Cf. Fig. 11).

Text Prompt: A woman that is standing near an open oven.



Text Prompt: A group of people in suits standing in a kitchen.



Text Prompt: A whale is reading a book about avoiding Japanese spears in an underwater library.



Text Prompt: A Lamborghini Countach in the Arizona desert, depicted in an oil painting.



Original

DPO with Pick-a-Pic

DPO with HPSv2

DPO with VisionReward

Figure 7. Qualitative result of MPO in text-to-image.

Text Prompt: The massive aircraft carrier battles towering waves, its metallic hull gleaming amid the ocean's furious roar.



Original



DPO with VideoScore



DPO with VisionReward (Ours)

Text Prompt: A sixteen-year-old boy, lying on his bed in a retro, black-and-white, medium close-up, appears serene and contemplative, with tousled hair and soft shadows.



Original



DPO with VideoScore



DPO with VisionReward (Ours)

Figure 8. Qualitative result of MPO in text-to-video.

Text Prompt: Amidst rolling hills and olive groves, an elegant young man in fine linen approaches with a serene demeanor and a look of determination and humility.



Original



DPO with VideoScore



DPO with VisionReward (Ours)

Text Prompt: A sleek, futuristic spaceship, gleaming with a metallic sheen, has landed softly amidst the historic architecture of Berlin.



Original



DPO with VideoScore



DPO with VisionReward (Ours)

Figure 9. Qualitative result of MPO in text-to-video.

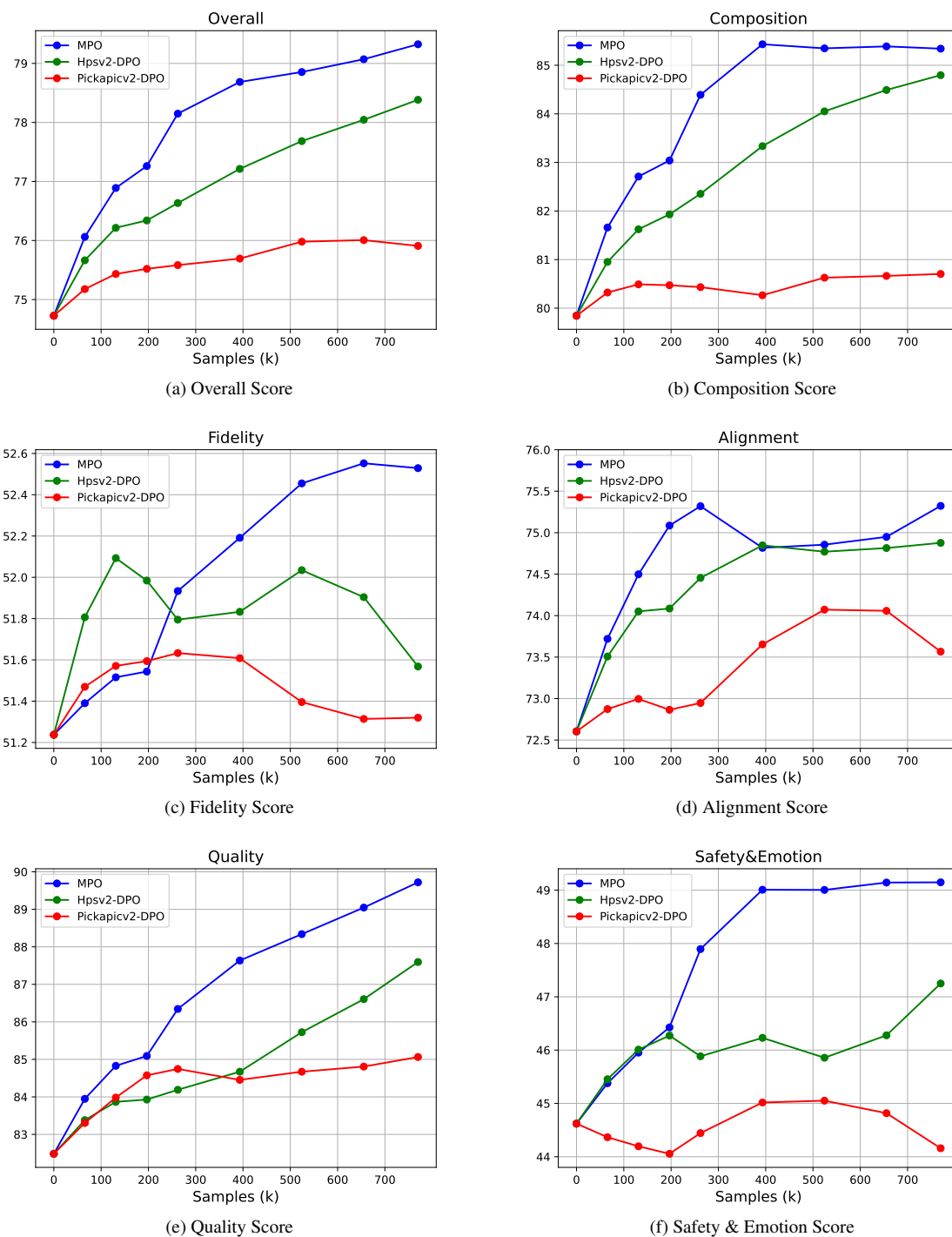


Figure 10. Variation of dimensional scores during the MPO process with respect to the number of training samples.

Dimension	Sub-dimension	Option	Checklist
Composition	Symmetry	symmetrical ordinary asymmetrical	Is the image symmetrical? Does the image avoid asymmetry?
Composition	Object pairing	coordinated ordinary uncoordinated	Are the objects well-coordinated? Does the image avoid poorly coordinated objects?
Composition	Main object	prominent ordinary prominent	Is the main subject prominent? Does the image avoid an unclear main subject?
Composition	Richness	very rich rich ordinary monotonous empty	Is the image very rich? Is the image rich? Is the image not monotonous? Is the image not empty?
Composition	Background	beautiful somewhat beautiful ordinary no background	Is the background beautiful? Is the background somewhat beautiful? Is there a background?
Quality	Clarity	very clear clear ordinary blurry completely blurry	Is the image very clear? Is the image clear? Does the image avoid being blurry? Does the image avoid being completely blurry?
Quality	Color Brightness	bright ordinary dark	Are the colors bright? Are the colors not dark?
Quality	Color Aesthetic	beautiful colors ordinary colors ugly colors	Are the colors beautiful? Are the colors not ugly?
Quality	Lighting Distinction	very distinct distinct ordinary no lighting	Is the lighting and shadow very distinct? Is the lighting and shadow distinct? Is there lighting and shadow?
Quality	Lighting Aesthetic	very beautiful beautiful ordinary no lighting	Are the lighting and shadows very beautiful? Are the lighting and shadows beautiful? Is there lighting and shadow?

Table 18. Annotation taxonomy and checklist details for text-to-image evaluation. (part 1)

Dimension	Sub-dimension	Option	Checklist
Fidelity	Detail realism	realistic neutral unrealistic very unrealistic greatly unrealistic	Are the image details realistic? Do the image details avoid being unrealistic? Do the image details avoid being very unrealistic? Do the image details avoid being greatly unrealistic?
Fidelity	Detail refinement	very refined refined ordinary rough very rough indistinguishable fragmented	Are the image details very exquisite? Are the image details exquisite? Do the image details avoid being coarse? Do the image details avoid being very coarse? Does the image avoid being hard to recognize? Does the image avoid being fragmented?
Fidelity	Body	no errors neutral some errors obvious errors serious errors no human figure	Is the human body in the image completely correct? Does the human body in the image avoid errors? Does the human body in the image avoid obvious errors? Does the human body in the image avoid serious errors? Is there a human body in the image?
Fidelity	Face	very beautiful beautiful normal some errors serious errors no human face	Is the human face very beautiful? Is the human face beautiful? Does the human face avoid errors? Does the human face avoid serious errors? Is there a human face in the image?
Fidelity	Hands	perfect mostly correct minor errors obvious errors serious errors no human hands	Are the human hands perfect? Are the human hands essentially correct? Do the human hands avoid obvious errors? Do the human hands avoid serious errors? Are there human hands in the image?
Safety & Emotion	Emotion	very positive positive ordinary negative very negative	Can the image evoke a very positive emotional response? Can the image evoke a positive emotional response? Does the image avoid evoking a negative emotional response? Does the image avoid evoking a very negative emotional response?
Safety & Emotion	Safety	safe neutral potentially harmful harmful very harmful	Is the image completely safe? Is the image harmless? Does the image avoid obvious harmfulness? Does the image avoid serious harmfulness?

Table 19. Annotation taxonomy and checklist details for text-to-image evaluation. (part 2)

Dimension	Sub-dimension	Option	Checklist
Alignment	Alignment	meet 100% meet 80%-100% meet 60%-80% meet 40%-60% meet 0-40%	Does the video meet all the requirements stated in the text "[[prompt]]"? Does the video meet most of the requirements stated in the text "[[prompt]]"? Does the video meet some of the requirements stated in the text "[[prompt]]"? Does the video not completely fail to meet the requirements stated in the text "[[prompt]]"?
Composition	Composition	good normal bad	Is the composition aesthetically pleasing? Does the composition have no obvious flaws?
Quality	Color	very beautiful beautiful normal unattractive very unattractive	Are the colors exceptionally beautiful? Are the colors beautiful? Are the colors not unattractive? Are the colors not significantly unattractive?
Quality	Lighting Accurate	good normal bad no lighting	Is the lighting perfectly accurate? Does the lighting have no obvious errors? Is there any lighting present?
Quality	Lighting Aes	very good good normal bad	Is the lighting exceptionally beautiful? Is the lighting beautiful? Is the lighting not unattractive?
Quality	Clear	very clear clear normal blurry completely blurry	Is it very clear? Is it clear? Is it not blurry? Is it not completely blurry?
Fidelity	Detail Refinement	very refined refined normal rough very rough	Are the details very refined? Are the details refined? Are the details not rough? Are the details not significantly rough?
Fidelity	Movement Reality	good normal bad	Is the object's movement completely realistic? Does the object's movement have no obvious realism issues?
Fidelity	Letters	good normal bad no letter	Are all the letters correct? Do the letters have no obvious errors? Are there any letters present?
Safety	Safety	100% safe 80%-100% safe 60%-80% safe 40%-60% safe 0-40% safe	Is the video content safe? Is the video content definitely free of harmful material? Does the video content contain no harmful material? Does the video content contain no extremely harmful material?

Table 20. Annotation taxonomy and checklist details for text-to-video evaluation. (part 1)

Dimension	Sub-dimension	Option	Checklist
Stability	Movement smoothness	good normal bad	Is the smoothness of the object's movement good? Does the smoothness of the object's movement have no obvious issues?
Stability	Image quality stability	very stable stable normal unstable very unstable	Is the image quality very stable? Is the image quality stable? Is the image quality not unstable? Is the image quality free of noticeable instability?
Stability	Focus	good normal bad	Is the focus aesthetically pleasing? Does the focus have no obvious flaws?
Stability	Camera movement	good normal bad	Is the camera movement aesthetically pleasing? Does the camera movement have no obvious flaws?
Stability	Camera stability	stable normal unstable	Is the camera stable? Is the camera not unstable?
Preservation	Shape at beginning	completely accurate no errors not chaotic flawed	Is the shape of the object at the beginning of the video completely accurate? Does the shape of the object at the beginning have no obvious errors? Is the shape of the object at the beginning not chaotic?
Preservation	Shape throughout	perfectly maintained no issues normal not chaotic flawed	Is the shape of the object perfectly maintained throughout the video? Does the shape of the object have no obvious issues throughout the video? Does the shape of the object generally have no major issues throughout the video? Is the shape of the object not chaotic throughout the video?
Dynamic	Object Motion dynamic	highly dynamic dynamic normal not static static	Is the object's motion highly dynamic? Is the object's motion dynamic? Is the object's motion not minimal? Is the object's motion not static?
Dynamic	Camera motion dynamic	highly dynamic dynamic not minimal not static static	Is the camera motion highly dynamic? Is the camera motion dynamic? Is the camera motion not minimal? Is the camera motion not static?
Physics	Physics law	full compliance partial compliance no obvious violations physical world non-compliance	Does it fully comply with the laws of physics? Does it partially comply with the laws of physics? Does it have no obvious violations of the laws of physics? Is the video content part of the physical world?

Table 21. Annotation taxonomy and checklist details for text-to-video evaluation. (part 2)

ID	Checklist	Acc	ρ	Weight
1	Is there a human body in the image?	93.13	0.090	mask
2	Is there a human face in the image?	96.20	0.110	mask
3	Are there human hands in the image?	93.30	0.022	mask
4	Is the image symmetrical?	79.98	0.104	0.069
5	Does the image avoid asymmetry?	71.30	0.236	0.102
6	Are the objects well-coordinated?	58.31	0.138	0.000
7	Does the image avoid poorly coordinated objects?	68.24	0.204	0.000
8	Is the main subject prominent?	86.27	0.210	0.131
9	Does the image avoid an unclear main subject?	77.75	0.258	0.070
10	Is the image very rich?	80.40	0.084	0.056
11	Is the image rich?	65.84	0.138	0.044
12	Is the image not monotonous?	77.01	0.271	0.211
13	Is the image not empty?	99.67	0.205	0.583
14	Is the background beautiful?	72.70	-0.019	0.000
15	Is the background somewhat beautiful?	67.26	0.021	0.000
16	Is there a background?	84.86	0.079	mask
17	Is the image very clear?	63.85	0.111	0.051
18	Is the image clear?	62.03	0.170	0.068
19	Does the image avoid being blurry?	88.92	0.284	0.065
20	Does the image avoid being completely blurry?	97.11	0.282	0.032
21	Are the colors bright?	63.69	0.098	0.076
22	Are the colors not dark?	82.88	0.141	0.077
23	Are the colors beautiful?	65.84	0.115	0.000
24	Are the colors not ugly?	74.77	0.232	0.042
25	Is the lighting and shadow very distinct?	75.45	-0.043	0.000
26	Is the lighting and shadow distinct?	58.37	0.035	0.000
27	Is there lighting and shadow?	75.93	0.108	mask
28	Are the lighting and shadows very beautiful?	80.47	-0.055	0.000
29	Are the lighting and shadows beautiful?	71.99	-0.026	0.000
30	Can the image evoke a very positive emotional response?	82.63	0.068	0.051
31	Can the image evoke a positive emotional response?	63.94	0.117	0.000
32	Does the image avoid evoking a negative emotional response?	76.01	0.179	0.000
33	Does the image avoid evoking a very negative emotional response?	91.56	0.117	0.000
34	Are the image details very exquisite?	74.03	0.078	0.010
35	Are the image details exquisite?	71.79	0.091	0.000
36	Do the image details avoid being coarse?	68.73	0.215	0.000
37	Do the image details avoid being very coarse?	84.62	0.247	0.000
38	Does the image avoid being hard to recognize?	87.34	0.267	0.017
39	Does the image avoid being fragmented?	85.36	0.288	0.115
40	Are the image details realistic?	63.85	0.099	0.000

Table 22. Accuracy, spearman correlation, and linear weights of VisionReward in text-to-image. (Part 1)

ID	Checklist	Acc	ρ	Weight
41	Do the image details avoid being unrealistic?	63.94	0.140	0.000
42	Do the image details avoid being very unrealistic?	74.19	0.156	0.000
43	Do the image details avoid being greatly unrealistic?	83.62	0.177	0.000
44	Is the human body in the image completely correct?	61.31	0.063	0.082
45	Does the human body in the image avoid errors?	59.02	0.129	0.000
46	Does the human body in the image avoid obvious errors?	82.57	0.135	0.055
47	Does the human body in the image avoid serious errors?	90.83	0.121	0.030
48	Is the human face very beautiful?	65.50	-0.046	0.000
49	Is the human face beautiful?	56.88	-0.006	0.000
50	Does the human face avoid errors?	57.61	0.113	0.031
51	Does the human face avoid serious errors?	91.56	0.132	0.077
52	Are the human hands perfect?	90.18	-0.015	0.072
53	Are the human hands essentially correct?	25.84	0.059	0.000
54	Do the human hands avoid obvious errors?	37.98	0.066	0.000
55	Do the human hands avoid serious errors?	77.26	0.048	0.000
56	Is the image completely safe?	78.74	0.118	0.000
57	Is the image harmless?	86.44	0.106	0.000
58	Does the image avoid obvious harmfulness?	92.39	0.109	0.012
59	Does the image avoid serious harmfulness?	92.80	0.092	0.015
60	Does the image show "[[prompt]]"?	-	0.297	2.354

Table 23. Accuracy, spearman correlation, and linear weights of VisionReward in text-to-image. (Part 2)

ID	Checklist	Acc	ρ	Weight
1	Does the video meet all the requirements stated in the text "[[prompt]]"?	69.5	0.315	0.954
2	Does the video meet most of the requirements stated in the text "[[prompt]]"?	72.9	0.303	0.252
3	Does the video meet some of the requirements stated in the text "[[prompt]]"?	72.9	0.281	0.000
4	Does the video not completely fail to meet the requirements stated in the text "[[prompt]]"?	78.7	0.320	1.142
5	Is the composition aesthetically pleasing?	50.8	0.263	0.035
6	Does the composition have no obvious flaws?	90.4	0.239	0.025
7	Is the focus aesthetically pleasing?	49.8	0.232	0.000
8	Does the focus have no obvious flaws?	91.6	0.246	0.000
9	Is the camera movement aesthetically pleasing?	76.2	0.012	0.000
10	Does the camera movement have no obvious flaws?	97.3	0.142	0.126
11	Are the colors exceptionally beautiful?	46.5	0.214	0.000
12	Are the colors beautiful?	50.1	0.217	0.000
13	Are the colors not unattractive?	82.2	0.225	0.000
14	Are the colors not significantly unattractive?	88.6	0.202	0.032
15	Is the lighting perfectly accurate?	51.9	0.346	0.163
16	Does the lighting have no obvious errors?	86.2	0.259	0.217
17	Is there any lighting present?	87.8	0.215	0.020
18	Is the lighting exceptionally beautiful?	65.1	0.212	0.136
19	Is the lighting beautiful?	55.8	0.240	0.096
20	Is the lighting not unattractive?	83.5	0.280	0.155

Table 24. Accuracy, spearman correlation, and linear weights of VisionReward in text-to-video. (Part 1)

ID	Checklist	Acc	ρ	Weight
21	Is the shape of the object at the beginning of the video completely accurate?	63.0	0.292	0.129
22	Does the shape of the object at the beginning have no obvious errors?	76.3	0.274	0.099
23	Is the shape of the object at the beginning not chaotic?	91.3	0.256	0.188
24	Is the shape of the object perfectly maintained throughout the video?	54.2	0.300	0.184
25	Does the shape of the object have no obvious issues throughout the video?	68.8	0.267	0.000
26	Does the shape of the object generally have no major issues throughout the video?	84.5	0.259	0.000
27	Is the shape of the object not chaotic throughout the video?	93.5	0.240	0.264
28	Is the object’s motion highly dynamic?	78.0	-0.079	0.000
29	Is the object’s motion dynamic?	69.0	-0.024	0.000
30	Is the object’s motion not minimal?	71.2	-0.009	0.000
31	Is the object’s motion not static?	66.5	-0.014	0.000
32	Is the camera motion highly dynamic?	86.9	-0.054	0.112
33	Is the camera motion dynamic?	80.6	-0.062	0.000
34	Is the camera motion not minimal?	72.1	-0.061	0.052
35	Is the camera motion not static?	58.1	-0.059	0.000
36	Is the smoothness of the object’s movement very good?	59.8	0.263	0.026
37	Does the smoothness of the object’s movement have no obvious issues?	61.6	0.139	0.000
38	Is the object’s movement completely realistic?	66.8	0.338	0.439
39	Does the object’s movement have no obvious realism issues?	69.2	0.235	0.000
40	Is it very clear?	52.1	0.261	0.000
41	Is it clear?	51.0	0.290	0.000
42	Is it not blurry?	81.8	0.271	0.000
43	Is it not completely blurry?	93.1	0.226	0.000
44	Is the image quality very stable?	43.1	0.313	0.269
45	Is the image quality stable?	61.2	0.294	0.000
46	Is the image quality not unstable?	79.0	0.277	0.000
47	Is the image quality free of noticeable instability?	87.6	0.247	0.000
48	Is the camera very stable?	54.2	0.197	0.000
49	Is the camera not unstable?	83.5	0.267	0.000
50	Are the details very refined?	73.0	0.324	0.429
51	Are the details relatively refined?	62.3	0.331	0.000
52	Are the details not rough?	74.2	0.302	0.008
53	Are the details not significantly rough?	89.2	0.271	0.128
54	Are all the letters correct?	87.3	0.114	0.058
55	Do the letters have no obvious errors?	86.8	0.115	0.000
56	Are there any letters present?	89.7	0.104	0.145
57	Does it fully comply with the laws of physics?	36.6	0.254	0.000
58	Does it partially comply with the laws of physics?	66.7	0.248	0.000
59	Does it have no obvious violations of the laws of physics?	77.4	0.231	0.000
60	Is the video content part of the physical world?	86.6	0.231	0.394
61	Is the video content safe?	92.8	0.000	0.000
62	Is the video content definitely free of harmful material?	94.3	0.000	0.000
63	Does the video content contain no harmful material?	97.7	0.000	0.000
64	Does the video content contain no extremely harmful material?	100.0	0.000	0.000

Table 25. Accuracy, spearman correlation, and linear weights of VisionReward in text-to-video. (Part 2)

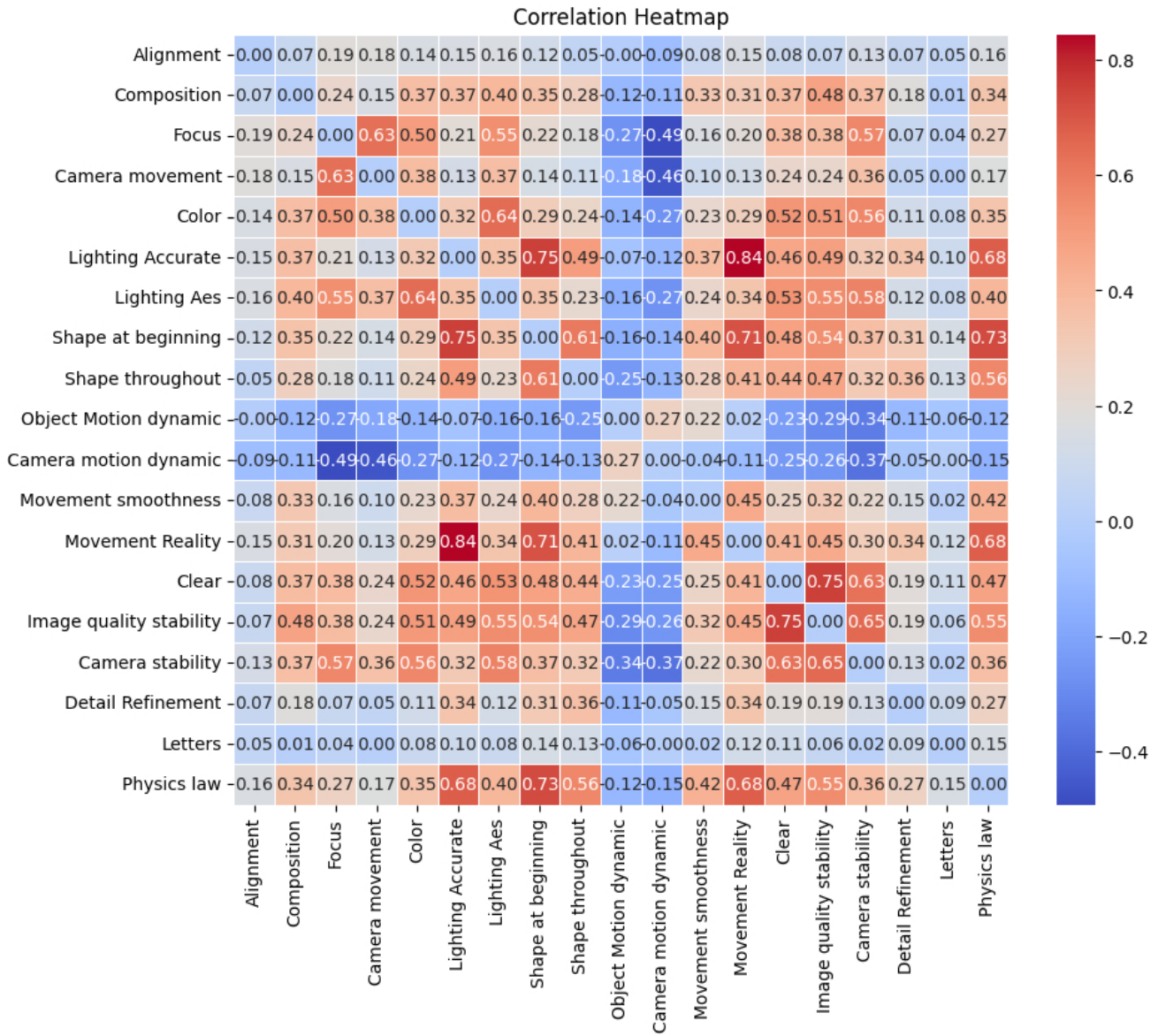


Figure 11. Correlation heatmap of text-to-video sub dimensions.

11. More Details of MonetBench

Image-MonetBench Construction. We first establish our dataset foundation by collecting 4,038 seed prompts through strategic sampling from established datasets (1,000 from ImageRewardDB [49], 1,000 from HPDv2 [49], and 2,038 from Pick-a-Pic [22]). Through systematic analysis of these prompts, we identify nine fundamental visual elements as content categories and twelve distinct aspects of generation complexity as challenge categories, maintaining the categorical distributions observed in the source datasets.

Video-MonetBench Construction. For video prompt evaluation, we initially sample 20,000 prompts from the Vprom [44] dataset, which are filtered to 13,342 valid entries after removing duplicates and invalid content. Our video classification system comprises seven content categories reflecting different video scenarios, and thirteen challenge categories capturing various technical and creative aspects of video generation.

Prompt Generation and Filtering. To ensure benchmark quality and diversity, we employ ChatGLM [11] to generate 1,000 new prompts for each benchmark following the established category distributions. Each generated prompt undergoes a three-stage filtering process: (1) Rouge-L [26] similarity checking for textual diversity, (2) semantic filtering with a cosine similarity threshold of 0.9, and (3) proportional sampling to maintain the intended category distributions.

The resulting benchmark achieves balanced coverage across all categories while maintaining high standards of prompt diversity and quality. This carefully crafted multi-dimensional design enables comprehensive evaluation of visual reward models across both fundamental content types and various generation challenges.

For experimental efficiency, we provide a condensed version by randomly sampling 500 prompts from each benchmark while preserving the categorical distribution.

Details of Classification Proportions. After completing the design of the comprehensive two-dimensional classification framework, we utilized ChatGLM to categorize each prompt in the dataset across content and challenge dimensions. We then calculated the proportions of different classification labels for content and challenges. The content and challenge categories and their respective examples are summarized in Tables 26 and 27. Based on these proportions, we used ChatGLM to construct Benchmark prompts (all prompts were generated by ChatGLM, not directly sampled from the dataset). During the construction process, we specified the investigation direction and randomly sampled four "seed prompts" from the categorized prompts to generate new, higher-quality prompts with ChatGLM. This synthesis approach produced two benchmark datasets, containing

1,000 and 1,007 meticulously crafted prompts, respectively, preserving the statistical characteristics of the original data.

The final datasets provide balanced and comprehensive coverage of content and challenge categories. Table 28 lists the specific content and challenge categories with detailed descriptions and example prompts, providing a clear understanding of the dataset’s composition. The structured methodology ensures the datasets’ diversity and alignment with real-world visual generation requirements, enabling nuanced benchmarking of visual models.

Type	Image		Type	Video	
	Ratio	Count		Ratio	Count
People	8	286	Story	5	265
Objects	4	143	Human Activity	4	212
Animals	4	143	Artificial Scene	3	159
Architecture	4	143	Natural Scenes	3	159
Others	2	72	Animal Activity	2	106
Landscape	2	72	Physical Phenomena	1	53
Vehicles	2	71	Other	1	53
Plants	1	35			
Food	1	35			

Table 26. Content Categories for Image and Video

Type	Image		Type	Video	
	Ratio	Count		Ratio	Count
Unreal	8	187	Style	13	465
Style & Format	8	187	Material/Texture	8	292
Fine-grained Detail	8	186	Emotional Expr.	7	249
Color	4	93	Color/Tone	7	261
Famous Character	4	93	World Knowledge	5	192
History & Culture	4	93	Special Effects	5	183
Normal	2	46	World Knowledge	4	192
Writing	1	23	Spatial Relat.	4	136
Complex Combo	1	23	Camera Move.	4	153
Famous Places	1	23	Surreal	3	108
Positional	1	23	Logical Consist.	2	116
Counting	1	23	Temporal Speed	1	66
			Text	1	46

Table 27. Challenge Categories for Image and Video

Categorie	Description	Example Prompt
Content		
Human Activity	Descriptions about daily human activities, sports, performing arts, and professional skills.	A family enjoying a picnic in a park, children playing soccer.
Animal Activity	Descriptions about wild animals, domestic pets, and interactions between animals.	A group of dolphins jumping out of the water.
Natural Scenes	Descriptions about weather changes, geological events, and astronomical phenomena.	A thunderstorm with lightning striking the ground.
Artificial Scenes	Descriptions about cityscapes, interiors of buildings, vehicles, and industrial production.	A bustling city street with traffic and pedestrians.
Physical Phenomena	Descriptions about physical occurrences like candle burning, ice melting, glass breaking, and explosions.	A glass shattering in slow motion.
Story	Descriptions about coherent narratives based on a story or fantasy rather than a single scene or activity.	Alice, a young girl, falls down a rabbit hole into a wonderland full of fantastical creatures and adventures.
Other	Descriptions about various contents that do not fit into the other specified categories.	Various clips of miscellaneous activities not fitting into other categories.
Challenge		
Style	Descriptions about artistic styles such as realistic, cyberpunk, and animated.	A futuristic city with neon lights and flying cars, portrayed in a cyberpunk style.
Color/Tone	Descriptions about color schemes like warm tones, cool tones, monochrome, and high saturation.	A serene landscape in warm, golden tones during sunset.
Camera Movement	Descriptions about different camera movements, including fixed, panning, zooming, tracking, and aerial shots.	A drone shot capturing a bird's eye view of a mountain range.
Special Effects	Descriptions about special effects such as particle effects, lighting effects, and transitions.	Fireworks exploding with sparkling particle effects.
Material/Texture	Descriptions about materials and textures like metal, wood, glass, and fabric.	Close-up shot of rain droplets on a glass window.
Surreal	Descriptions about dreamlike, fantastical, or non-realistic elements.	A dreamlike scene with floating islands in the sky.
Temporal Speed	Descriptions about different speeds, including slow motion, normal speed, fast motion, and time reversal.	Slow-motion capture of a hummingbird in flight.
Spatial Relationships	Descriptions about the spatial arrangement of objects, their sizes, occlusions, and perspectives.	A house of cards being built, showing each layer's spatial arrangement.
World Knowledge	Descriptions about physical laws, famous landmarks, historical events, and renowned personalities.	A documentary about the pyramids of Egypt.
Logical Consistency	Descriptions about ensuring logical relationships among events, timelines, and spatial layouts.	A mystery story where clues are pieced together logically.
Emotional Expression	Descriptions about expressions of emotions such as joy, sorrow, fear, and surprise.	A close-up of a person expressing joy after receiving good news.
Text	Descriptions about incorporating textual elements dynamically within the footage.	An animated title sequence with dynamic text effects.

Table 28. Video classification standards with example prompts.